Numerical Investigations of Model Scramjet Combustors

Markus Kindler, Thomas Blacha, Markus Lempke, Peter Gerlinger, and Manfred Aigner

Institut für Verbrennungstechnik der Luft- und Raumfahrt, Universität Stuttgart
Pfaffenwaldring 38-40, 70569 Stuttgart, Germany

Summary. In the present paper different types of scramjet (supersonic combustion ramjet) combustors are investigated. Thereby the main difference between the combustors is the way of injecting the fuel into the combustion chamber. The first investigated concept of fuel injection is the injection by strut injectors. Here the injection of fuel is realized by a lobed strut that is located in the middle of the combustion chamber. The second concept for fuel supply is the wall injection of hydrogen. Here the fuel is injected by several holes in the wall of the combustor. Both concepts of fuel injection have different advantages and disadvantages which are explained in detail. Although different performance parameters for both scramjet combustors are introduced this paper will not compare the different techniques among each other. Because of the high Reynolds numbers in scramjet combustors, the need to resolve the boundary layers and the necessity of detailed chemistry, the simulation of scramjets is extremely CPU time demanding.

1 Introduction

Due to the high velocities in a scramjet combustor the residence time of air and fuel in the combustion chamber is extremely short. Additionaly the mixing rates at high flow Mach numbers are inherently low. Hence techniques are required to achieve a rapid and efficient mixing of fuel and air and thus a stable combustion and a complete burnout of the fuel. There are mainly two concepts of fuel injection: 1. wall injectors [1, 2, 3] and 2. strut injectors [4, 5, 6, 7]. In case of a wall injection the fuel is injected through the wall into the air flow. Wall injectors are easy to manufacture and easy to cool, have a good near field mixing and cause no pressure loss when they are turned off. On the other hand in real size combustors there might be problems of the penetration depth of the fuel into the air flow and a strong blockage might occur in the combustion chamber. Strut injectors, where the fuel is injected through a strut directly into the core of the air flow, cannot be removed from the flow and hence cause pressure losses even when they are switched off.

Additionally they have to be cooled and usually need mixing enhancement techniques. The advantages of strut injectors are the absence of strong shock waves due to a blockage caused by the fuel jet. In the present paper both concepts are investigated numerically.

2 Governing Equations and Numerical Scheme

The scientific inhouse code TASCOM3D (Turbulent All Speed Combustion Multigrid) describes reacting flows by solving the full compressible Navier-Stokes, species and turbulence transport equations. Additionally an assumed PDF (probability density function) approach is used to take turbulence chemistry interaction into consideration. Therefore two additional equations (for the variance of the temperature and the variance of the sum of species mass fractions) have to be solved. Thus the described set of averaged equations in three-dimensional conservative form is given by

$$\frac{\partial \mathbf{Q}}{\partial t} + \frac{\partial (\mathbf{F} - \mathbf{F}_\nu)}{\partial x} + \frac{\partial (\mathbf{G} - \mathbf{G}_\nu)}{\partial y} + \frac{\partial (\mathbf{H} - \mathbf{H}_\nu)}{\partial z} = \mathbf{S}\,, \tag{1}$$

where

$$\mathbf{Q} = \left[\bar{\rho}, \bar{\rho}\tilde{u}, \bar{\rho}\tilde{v}, \bar{\rho}\tilde{w}, \bar{\rho}\tilde{E}, \bar{\rho}q, \bar{\rho}\omega, \bar{\rho}\sigma_T, \bar{\rho}\sigma_Y, \bar{\rho}\tilde{Y}_i\right]^T, \quad i = 1, 2, \ldots, N_k - 1\,. \tag{2}$$

The variables in the conservative variable vector $\mathbf{Q}$ are the density $\bar{\rho}$ (averaged), the velocity components (Favre averaged) $\tilde{u}$, $\tilde{v}$ and $\tilde{w}$, the total specific energy $\tilde{E}$, the turbulence variables $q = \sqrt{k}$ and $\omega = \epsilon/k$ (where k is the kinetic energy and ϵ the dissipation rate of k), the variance of the temperature σ_T and the variance of the sum of the species mass fractions σ_Y and finally the species mass fractions Y_i ($i = 1, 2, \ldots, N_k - 1$). Thereby N_k describes the total number of species that are used for the description of the gas composition. The vectors $\mathbf{F}$, $\mathbf{G}$ and $\mathbf{H}$ specify the inviscid fluxes in x-, y- and z- direction, $\mathbf{F}_\nu$, $\mathbf{G}_\nu$ and $\mathbf{H}_\nu$ the viscous fluxes, respectively. The source vector $\mathbf{S}$ in Eq. (1) results from turbulence and chemistry and is given by

$$\mathbf{S} = \left[0, 0, 0, 0, 0, \bar{S}_q, \bar{S}_\omega, \bar{S}_{\sigma_T}, \bar{S}_{\sigma_Y}, \bar{S}_{Y_i}\right]^T, \quad i = 1, 2, \ldots, N_k - 1\,, \tag{3}$$

where $\bar{S}_q$ and $\bar{S}_\omega$ are the averaged source terms of the turbulence variables, $\bar{S}_{\sigma_T}$ and $\bar{S}_{\sigma_Y}$ the source terms of the variance variables (σ_T and σ_Y) and $\bar{S}_{Y_i}$ the source terms of the species mass fractions. For turbulence closure a two-equation low-Reynolds-number q-ω turbulence-model is applied [8]. The momentary chemical production rate of species i in Eq. (1) is defined by

$$S_{Y_i} = M_i \sum_{r=1}^{N_r} \left[\left(\nu_{i,r}^{''} - \nu_{i,r}^{'} \right) \left(k_{fr} \prod_{l=1}^{N_k} c_l^{\nu_{l,r}^{'}} - k_{br} \prod_{l=1}^{N_k} c_l^{\nu_{l,r}^{''}} \right) \right], \tag{4}$$

where k_{f_r} and k_{b_r} are the forward and backward rate constants of reaction r (defined by the Arrhenius function), the molecular weight of a species M_i, the species concentration $c_i = \rho Y_i / M_i$ and the stoichiometric coefficients $\nu'_{i,r}$ and $\nu''_{i,r}$ of species i in reaction r. The averaged chemical production rate for a species i due to the use of the assumed PDF approach and the assumption of statistical independence of temperature, gas composition and density is given by

$$\bar{S}_{Y_i} = \int S_i \left(\hat{T}, \hat{c}_1, \cdots, \hat{c}_{N_k}\right) P \left(\hat{T}, \hat{c}_1, \cdots, \hat{c}_{N_k}\right) d\hat{T} d\hat{c}_1 \cdots d\hat{c}_{N_k} \,, \tag{5}$$

where

$$P \left(\hat{T}, \hat{c}_1, \cdots, \hat{c}_{N_k}\right) = P_T \left(\hat{T}\right) P_Y \left(\hat{Y}_1, \cdots, \hat{Y}_{N_k}\right) \delta \left(\hat{\rho} - \bar{\rho}\right) \,. \tag{6}$$

P_T defines the temperature PDF desribed by a Gaussian distribution

$$P_T \left(\hat{T}\right) = \frac{1}{\sqrt{2\pi\sigma_T}} \exp \left[- \frac{\left(\hat{T} - \widetilde{T}\right)^2}{2\sigma_T} \right] \,, \quad \sigma_T = \widetilde{T''^2} \tag{7}$$

that is clipped at lower and upper temperature limits due to the limitations of the Arrhenius equation [9]. The PDF of the gas composition P_Y is described by the multi-variate β-pdf proposed by Girimaji [10]

$$P_Y \left(\hat{Y}_1, \cdots, \hat{Y}_{N_k}\right) = \frac{\Gamma \left(\sum_{m=1}^{N_k} \beta_m\right)}{\prod_{m=1}^{N_k} \Gamma \left(\beta_m\right)} \left[\delta \left(1 - \sum_{m=1}^{N_k} \hat{Y}_m \right) \prod_{m=1}^{N_k} \hat{Y}_m^{\beta_m - 1} \right] \tag{8}$$

where

$$\beta_m = \tilde{Y}_m B, \quad B = \left[\frac{\sum_{m=1}^{N_k} \widetilde{Y}_m \left(1 - \widetilde{Y}_m\right)}{\sigma_Y} - 1 \right] \,, \quad \sigma_Y = \sum_{m=1}^{N_k} \widetilde{Y''^2_m} \,. \tag{9}$$

δ in Eq. (6) and (8) denotes the δ-function. The unsteady set of equations (1) is solved using an implicit Lower-Upper-Symmetric Gauss-Seidel (LU-SGS) [11, 12, 13, 14] finite-volume algorithm, where the finite-rate chemistry is treated fully coupled with the fluid motion. More details concerning TASCOM3D may be found in [13, 14, 15, 16, 17, 18]

3 Investigations of Lobed Strut Injectors

In this section a scramjet combustion chamber with a strut injector is investigated. Main focus is the effect of different amounts of circulation produced by the lobed strut on the mixing and hence on the combustion process. Thereby hydrogen is injected in axial flow direction by a lobed strut injector (see Fig. 1)

which creates streamwise vortices to enhance the mixing (compared to planar struts) [19]. In order to produce different amounts of circulation the length of the lobed structure of the strut is varied. Fig. 1 shows the struts investigated which all have 60 mm in width and 8 mm in height, while the length of the lobed parts differ. The area for hydrogen injection is the same in all three cases.

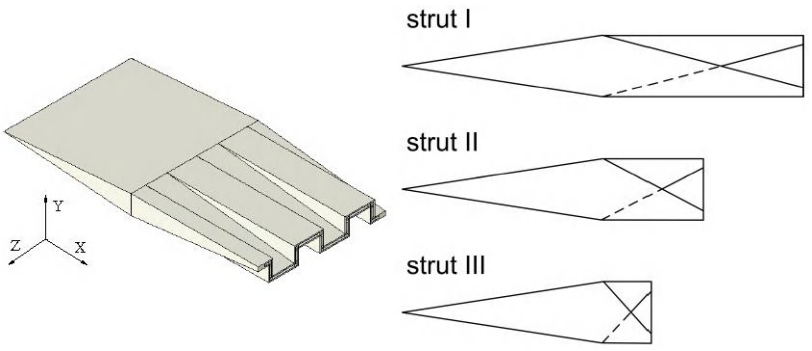

Fig. 1. Investigated struts with different lengths and amount of vorticity production

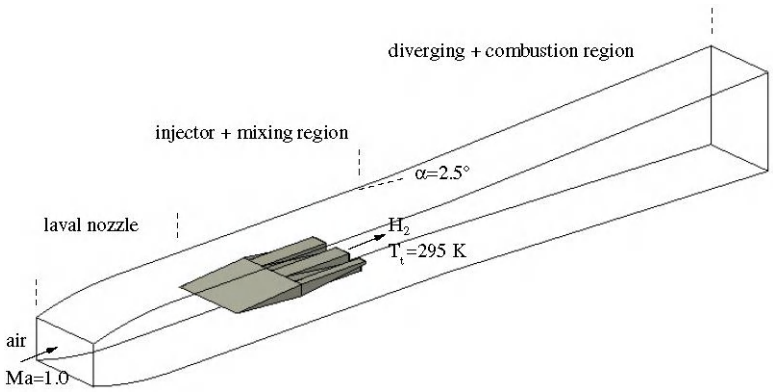

Fig. 2. Sketch of the combustion chamber with a lobed strut injector

In case of strut I the length is 80 mm. For strut II the lobed part is shortened by a factor of 2 (60 mm total length) and for strut III by a factor of 4 in comparison to strut I (50 mm total length). A reduction of the strut length increases the angles for changes in flow direction and thus the strength of the expansion fans at the middle of the strut and the pressure ratio in

cross stream direction. Thus the shorter struts create stronger vortices. Fig. 2 demonstrates a sketch of the combustion chamber with a lobed strut injector. The dimensions of the combustor are 536 mm x 60 mm x 38 mm. Thereby the computional domain includes only a section of the combustion chamber using periodic and symmetry boundary comditions. Furthermore the simulations have been performed in two steps: a two-dimensional simulation up to the middle of the strut and three-dimensional simulations of the remaining combustion chamber. The inflow conditions for the simulations are summarized in Tab. 1. More details concerning the model scramjet combustor geometry and the lobed strut injectors may be found in [20]. The grid of the computational domain has about 800.000 volumes (220 x 70 x 54) and is strongly refined at all near wall regions as well as in the main combustion zone. Although the quantity of the volumes is moderate the computational costs are high due to the additional transport equations for the variances and especially the species as well as the numerical stiffness caused by combustion. Fig. 3 shows representatively for all configurations the H_2O, H_2 and OH distributions of the model scramjet combustor using strut I, respectively. The hydrogen distribution nicely shows the production of vortices due to the lobed strut injector right after the injection. The H_2O and OH distributions represent the combustion process and show that in all cases (strut I - strut III) lifted flames are obtained. As observed in previous investigations [19], ignition takes place near the point where the diverging channel part begins. The positions for ignition vary between 85 mm (strut I), 105 mm (strut II) and 110 mm (strut III), respectively. Further downstream the flame becomes wider and the separated structures grow together till the flame has a W-shape at the outlet of the combustion chamber. In order to describe the effect of the struts on the combustion process calculated H_2O distributions are plotted in Fig. 4 for different y-z slices at channel positions ranging from 100-400 mm. 100 mm downstream of the hydrogen injection the shortest strut has a very small amount of H_2O, because ignition has just occured. In case of the longest

Table 1. Inflow conditions for the simulation of the combustion chamber with the lobed strut injector

	air	strut
pressure p [Pa]	211000	50000
temperature T [K]	1300	196
velocity u $[\frac{m}{s}]$	723	2281
Mach-number Ma [-]	1	2
mass fraction Y_{H_2}	0	1
mass fraction Y_{O_2}	0.23	0
mass fraction Y_{N_2}	0.77	0
$\dot{m}$ $[\frac{g}{s}]$	628	4.18

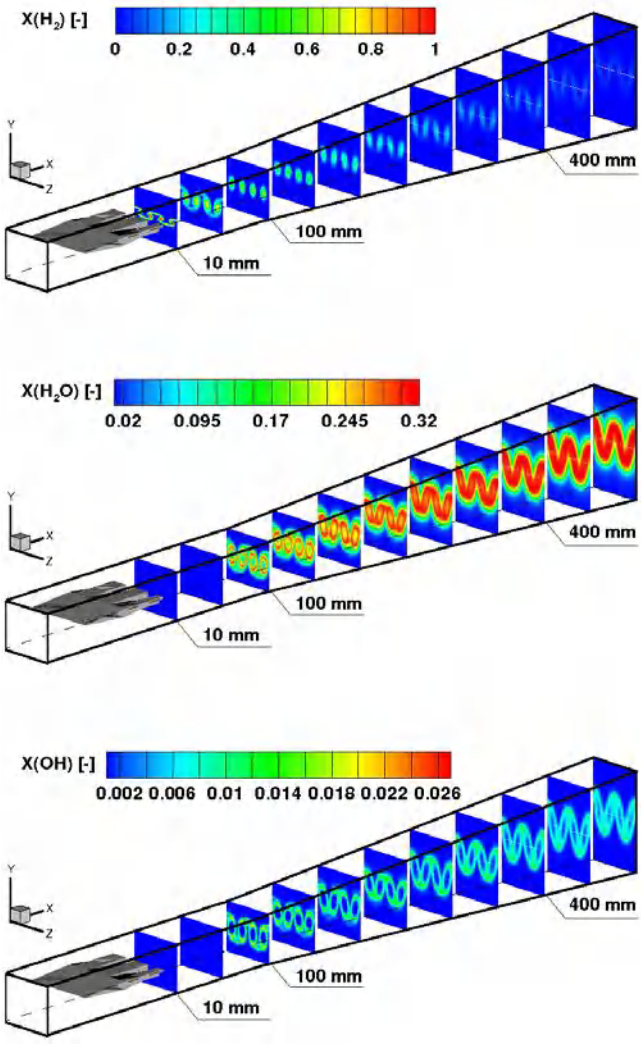

Fig. 3. Calculated H_2, H_2O and OH distributions (from top to bottom) of the model scramjet combustor using strut I, respectively

strut the combustion process is already in progress and the amount of H_2O is much higher compared to the other struts. The main combustion zone in all three cases forms two circles which are turning to a more elliptical shape with an increased strut length. With increasing distance from the fuel injector the flame spreads in vertical direction and the circle-like shapes grow together. In case of the shortest strut the flame shows the most homogeneous H_2O distribution, whereas the differences are quite small at the end of the combustion

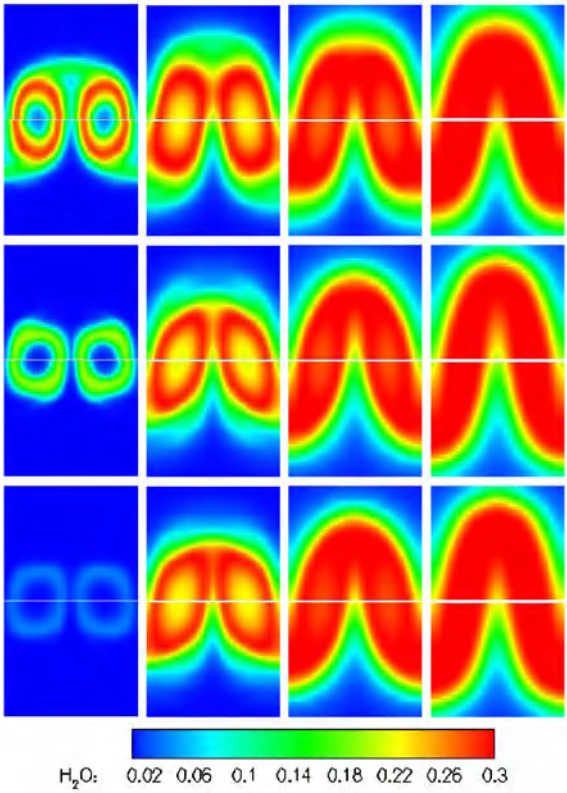

Fig. 4. Calculated H_2O molar fraction in y-z cross sections at x = 100, 200, 300, and 400 mm for the struts I to III (from top to bottom)

chamber. Finally in Fig. 5 a comparison of the three struts by means of performance parameters (hydrogen mass flux, total pressure) is given. Strut I has the best mixing in the near field of the injector which causes an early ignition and burning of the hydrogen (indicated by the rapid decrease of the hydrogen mass flux at the normalized channel length of 0.15). However, with increasing distance from the strut, vorticity seems to be too weak to transport air from the upper and lower channel walls into the main combustion zone. This results in a higher amount of unburned hydrogen at the end of the combustor compared with strut II and III. Strut III has the fewest amount of unburned hydrogen at the outlet. The differences in loss in total pressure between the three struts are relatively small.

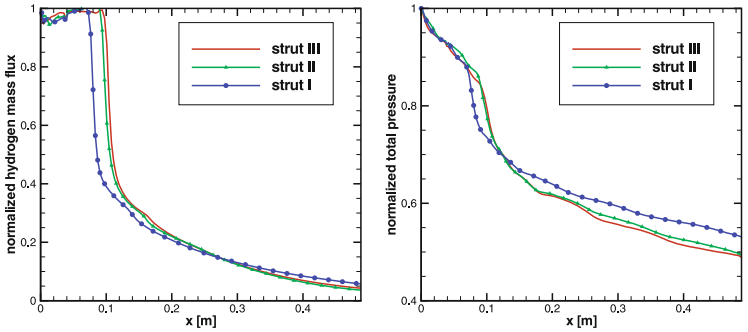

Fig. 5. Normalized hydrogen mass flux and total pressure over the normalized channel length for strut I to III, respectively

4 Investigations of Wall Injectors

In this section a scramjet combustion chamber with wall injection is investigated. Thereby the geometry and flow conditions are based on the HyShot flight experiments performed since 2001 by the University of Queensland to investigate supersonic combustion in flight. Since the beginning of the program four launches have been realized (HyShot I-IV) in which supersonic combustion has been achieved at HyShot II (2002) and HyShot III (2006). Additionally in the year 2003 and again in 2007 an identical model of the HyShot combustor has been investigated in the High Enthalpy Shock Tunnel in Göttingen (HEG) [21]. Thereby several freestream conditions, equivalence ratios and angles of attack have been investigated. Fig. 6 demonstrates a sketch of the combustion chamber. The flow approaches an intake ramp (363 x 100 mm) with a Mach-number of about 7.8. Due to the induced shocks

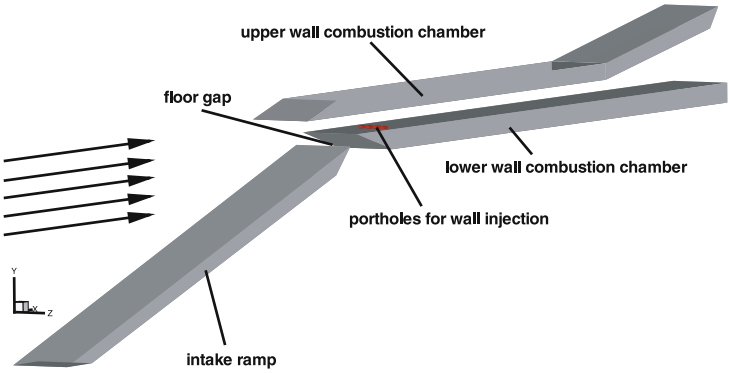

Fig. 6. Sketch of the combustion chamber with wall injectors

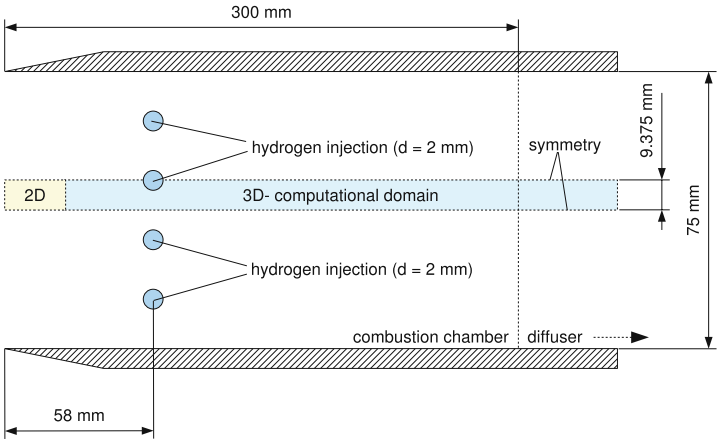

Fig. 7. Computational domain for the numerical simulation of the combustion chamber with wall injectors

at the leading edges of the intake ramp and the combustion chamber (300 x 75 x 9.8 mm) the flow reaches a Mach-number of 2.65 in front of the wall injectors. To ensure a relatively homogenous flow field in the combustion chamber the boundary layer is bled and shocks are by-passed through the floor gap indicated in Fig. 6. Again the numerical simulation has been performed in two steps: a two-dimensional simulation for the intake ramp and a three-dimensional simulation for the combustion chamber and the diffuser. The computational domain (Fig. 7) covers a slice from the middle of a wall injector to the symmetry line between two portholes using symmetry boundary conditions Thereby the grid of the computational domain has about 1.500.000 cell volumes. Tab. 2 summarizes the inflow conditions for the numerical sim-

Table 2. Inflow conditions for the simulation of the combustion chamber with the lobed strut injector

	air	wall injector
pressure p [bar]	1725	258135
temperature T [K]	221	250
velocity u $[\frac{m}{s}]$	2328	1250
Mach-number Ma [-]	7.8	1
mass fraction Y_{H_2}	0	1
mass fraction Y_{O_2}	0.23	0
mass fraction Y_{N_2}	0.77	0
$\dot{m}$ $[\frac{g}{s}]$	422.78	4.24

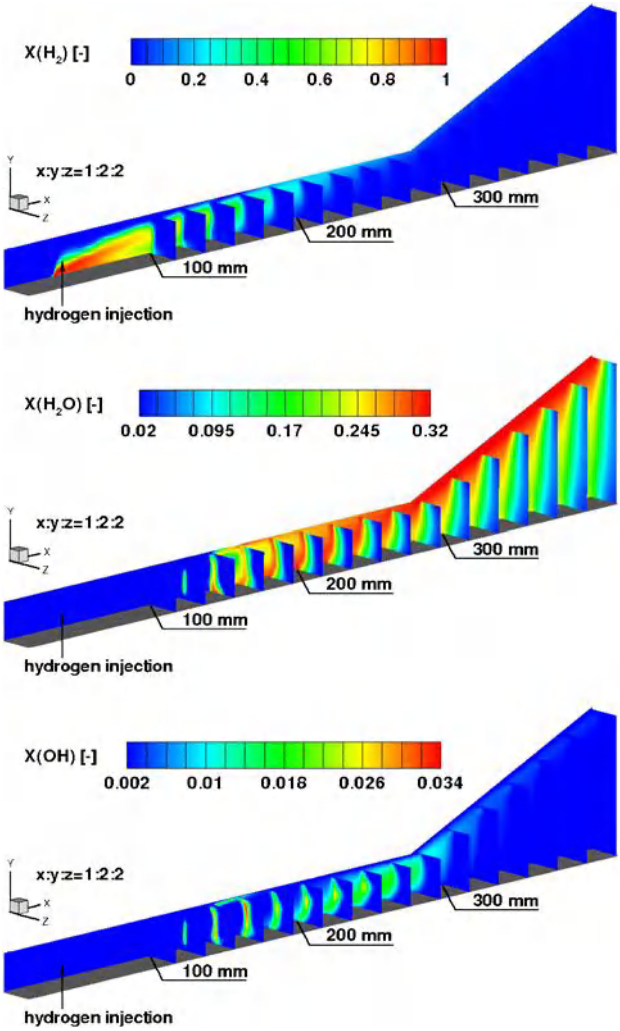

Fig. 8. Calculated H_2,H_2O and OH distribution (from top to bottom) of the HyShot scramjet combustor, respectively

ulation of the combustion chamber. Fig. 8 shows the calculated H_2, H_2O and OH distribution of the HyShot combustion chamber with hydrogen injection into air. A lifted flame is obtained and combustion starts about 60 mm downstream of the hydrogen injection. Fig. 8 shows in the beginning a relatively homogeneous hydrogen distribution in vertical direction. The majority of the unburned hydrogen at the end of the combustor (about 200-300 mm distance downstream of the combustor entrance) is located at the upper wall. The

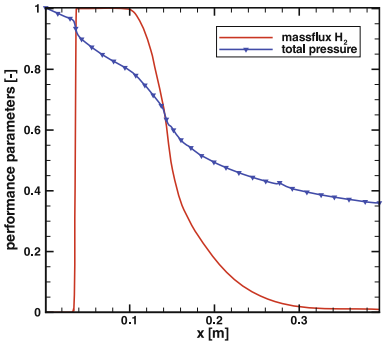

Fig. 9. Normalized hydrogen mass flux and total pressure over the channel length for the HyShot scramjet combustor, respectively

H_2O-distribution demonstrates that combustion starts at the outer regions of the area covered by hydrogen. After ignition the flame has a circle-like shape and turns to a relatively homogeneous distribution at a distance of about 200 mm from the combustor entrance. Further downstream the main combustion zone is located at the upper wall. Similar observation are obtained from the OH-distribution. Fig. 9 describes the normalized hydrogen mass flux and normalized total pressure along the channel length, respectively. Again the ignition delay can be identified by the rapid decrease of the hydrogen mass flux taking place at a distance of about 60 mm downstream of the fuel injection. At the combustor exit nearly no unburned fuel is left. The total pressure shows two dips: the first due to the injection of the hydrogen at about x = 0.04 m and the second due to the combustion process at about x = 0.11 m. The total pressure loss at the end of the combustion chamber is about 64% compared to the value at the combustor entrance.

5 Performance

Previous investigations of the performance of TASCOM3D on the NEC SX-8 [22] have shown that the performance in case of combustion simulations is quite good. Thereby a huge part of the whole computational time is consumed by a subroutine calculating PDF averaged chemical production rates and source term Jacobians. Due to the fact that chemistry is a local phenomena, a good vector lengths, quantity of MFLOPS and vector operation ratio are reached in the corresponding routine. Another huge part is consumed by the implicit solver used which is required because of the high numerical stiffness caused by combustion. The implicit solver is vectorized along diagonals (planes in 3D) to prevent data dependencies. The length of these diagonals depends on the size of the block and hence is dependent on the geometry

which could yield to relatively short vector lengths in blocks with few cells. In this paper additionally the MPI - parallelization of TASCOM3D has been reviewed and tested in order to achieve good performance in parallel runs. Therefore a testcase (i.e. two dimensional channel flow of an inert gas) with about 2.000.000 cell volumes has been calculated by a one block serial run and parallel runs with two, four and eight blocks, respectively. Tab. 3 shows the number of CPUs, the total CPU time consumed by the simulation, the averaged vector length and vector operation ratio as well as the MFLOPs reached for 1000 iterations. For the serial run TASCOM shows an excellent

Table 3. Perfomance parameter for simulation with 1, 2, 4 and 8 CPUs

CPUs [-]	total CPU-time [s]	aver. v.len [-]	v.op. ratio [-]	MFLOPS [-]
1	1008	243.9	99.2	6133.8
2	1079	242.7	99.09	5731.8
4	1165	234.8	99.01	5307.7
8	1473	205.8	98.80	4200.4

performance. The averaged vector length and vector operation ratio reaches nearly the maximum values and the total CPU-time is 1008 s. With increasing number of CPUs the total CPU-time raises up to 1473 s for 8 CPUs (which is a factor of 1.46). The main reason can be found in the averaged vector length which becomes shorter with increasing number of CPUs. The total number of cell volumes per CPU becomes smaller due to the fragmentation of the grid. Hence the diagonals for the implicit solver are shorter and thus the vector length. Therefore the number of cell volumes per CPU should be sufficient high in every simulation in order to reach a good performance. The problem of the shortening of vector lengths would be less dramatic in three-dimensional test-cases (which have not been investigated in this section) because the vector length significantly increases while the implicit solver vectorizes along planes compared to diagonals. Nevertheless the performance of the parallelization has to be investigated more detailed and further improved.

6 Conclusion

The scientific inhouse code TASCOM3D has been used to investigate different configurations of scramjet combustors. One investigated combustor configuration uses lobed strut injectors while the other configuration uses wall injection. In case of the lobed strut injection the effect of different amounts of circulation on the combustion process is investigated additionally. The code has been tested on the NEC SX-8 and has shown to have a good vector performance. Also the implemented MPI - parallelization has been tested on the NEC SX-8.

It has been shown that the number of cell volumes per CPU should be as high as possible in order to reach a good performance.

Acknowledgements

This work was performed within the 'Long-Term Advanced Propulsion Concepts and Technologies' project investigating high-speed airbreathing propulsion. LAPCAT, coordinated by ESA-ESTEC, is supported by the EU within the 6th Framework Programme Priority 1.4, Aeronautic and Space, Contract no.: AST4-CT-2005-012282. Further information on LAPCAT can be found on http://www.esa.int/techresources/lapcat The simulations were performed on the national super computer NEC SX-8 at the High Performance Computing Center Stuttgart (HLRS) under the grant number scrcomb.

References

1. Belanger, J., Hornung, H.G., Transverse Jet Mixing and Combustion Experiments in Hypervelocity Flows, Journal of Propulsion and Power, **12**, pp. 186-192, 1996.
2. Riggins, D.W., McClinton, C.R., Rogers, R.C., Bittner, R.D.: Investigation of Scramjet Injection Strategies for High Mach Number Flows, Journal of Propulsion and Power, 11, pp. 409-418, 1995.
3. Baurle, R.A., Fuller, R.P., White, J.A., Chen, T.H., Gruber, M.R., Nejad, A.S: An Investigation of Advanced Fuel Injection Schemes for Scramjet Combustion, AIAA paper 98-0937, 1998.
4. Glawe, D.D., Samimiy, M., Nejad, A.S., Cheng, T.H.: Effects of Nozzle Geometry on Parallel Injection from Base of an Extended Strut into a Supersonic Flow, AIAA paper 95-0522, 1995.
5. Strickland, J.H., Selerland, T., Karagozian, A.R: Numerical Simulation of a Lobed Fuel Injector, Physics of Fluids, 10, pp. 2950-2964, 1998.
6. Charyulu, B.V.N., Kurian, J., Venugopalan, P., Sriamulu, V.: Experimental Study on Mixing Enhancement in Two Dimensional Supersonic, Experiments in Fluids, 24, pp. 340-346, 1998.
7. Sunami, T., Wendt, M., Nishioka, M.: Supersonic Mixing and Combustion Control Using Streamwise Vorticity, AIAA paper 98-3271, 1998.
8. Coakley, T.J., Huang, P.G., Turbulence Modeling for High Speed Flows, AIAA paper 92-0436, 1992.
9. Gerlinger, P., Möbus, H., Brüggemann, D.: An Implicit Numerical Scheme for Turbulent Combustion Using an Assumed PDF Approach, AIAA paper 99-3775, 1999.
10. Girimaji, S.S.: A Simple Recipe for Modeling Reacting-Rates in Flows with Turbulent Combustions, AIAA paper 91-1792, 1991.
11. Jameson, A., Yoon, S.: Lower-Upper Implicit Scheme with Multiple Grids for the Euler Equations, AIAA Journal, **25**, pp. 929-937, 1987.
12. Shuen, J.S.: Upwind Differencing and LU Factorization for Chemical Non-Equilibrium Navier-Stokes Equations, Journal of Computational Physics, **99**, pp. 233-250, 1992.

13. Gerlinger, P., Brüggemann, D.: An Implicit Multigrid Scheme for the Compressible Navier-Stokes Equations with Low-Reynolds-Number Turbulence Closure, Journal of Fluids Engineering, **120**, pp. 257-262, 1998.
14. Gerlinger, P., Möbus, H., Brüggemann, D.: An Implicit Multigrid Method for Turbulent Combustion, Journal of Computational Physics, **167**, pp. 247-276, 2001.
15. Gerlinger, P., Brüggemann, D.: Numerical Investigation of Hydrogen Strut Injections into Supersonic Air Flows, Journal of Propulsion and Power, **16**, pp. 22-28, 2000.
16. Gerlinger, P.: Investigations of an Assumed PDF Approach for Finite-Rate-Chemistry, Combustion Science and Technology, **175**, pp. 841-872, 2003.
17. Stoll, P., Gerlinger, P., Brüggemann, D.: Domain Decomposition for an Impicit LU-SGS Scheme Using Overlapping Grids, AIAA-paper 97-1896, 1997.
18. Stoll, P., Gerlinger, P., Brüggemann, D.: Implicit Preconditioning Method for Turbulent Reacting Flows, Proceedings of the 4th ECCOMAS Conference, **1**, pp. 205-212, John Wiley & Sons, 1998.
19. Gerlinger, P., Stoll, P., Kindler, M., Schneider, F. and Aigner, M.: Numerical Investigation of Mixing and Combustion Enhancement in Supersonic Combustors by Strut Induced Ttreamwise Vorticity, Aerospace Science and Technology, **12**, pp. 159-168, 2008.
20. Kindler, M., Gerlinger, P. and Aigner, M.: Numerical Investigations of Mixing Enhancement by Lobed Strut Injectors in Turbulent Reactive Supersonic Flows, ISABE-2007-1314, 2007.
21. Gardner, A.: HyShot Scramjet Testing in the HEG,FB 2007-14,University of Queensland, Australia, 2007.
22. Kindler, M., Gerlinger, P. and Aigner, M.: Assumed PDF Modeling of Turbulence Chemistry Interaction in Scramjet Combustors, High Performance Computing in Science and Engineering '07, pp. 203-213, 2008.